Thin Solid Films 517 (2009) 6502–6507

Contents lists available at ScienceDirect

Thin Solid Films

journal homepage: www.elsevier.com/locate/tsf

Structural and mechanical properties of diamond-like carbon films deposited by an anode layer source

Markus Kahn [a,*], Miha Čekada [b], Thomas Schöberl [c], Roswitha Berghauser [a], Christian Mitterer [d], Christoph Bauer [e], Wolfgang Waldhauser [a], Elmar Brandstätter [a]

[a] Joanneum Research, Laser Center Leoben, Leobner Strasse 94, A-8712 Niklasdorf, Austria
[b] Jožef Stefan Institute, Department of Thin Films and Surfaces, Jamova 39, 1000 Ljubljana, Slovenia
[c] Erich Schmid Institute of Materials Science of the Austrian Academy of Sciences, Jahnstrasse 12, A-8700 Leoben, Austria
[d] University of Leoben, Department of Physical Metallurgy and Materials Testing, Franz-Josef Strasse 18, A-8700 Leoben, Austria
[e] University of Graz, Institute of Earth Sciences, Department of Mineralogy and Petrology, Universitätsplatz 2, A-8010 Graz, Austria

ARTICLE INFO

Article history:
Received 17 July 2008
Received in revised form 25 March 2009
Accepted 27 March 2009
Available online 6 April 2009

Keywords:
Diamond-like carbon (DLC)
Linear ion beam source
Mechanical properties
Raman spectroscopy

ABSTRACT

An anode layer source is a special ion gun, which can be fed with carbon precursors like acetylene to deposit hard and highly defect-free hydrogenated diamond-like carbon films at room temperature. The present study focuses on the influence of the process parameters — discharge voltage, process pressure and acetylene flow — on structure and mechanical properties of the deposited films. Raman spectra show that an increased discharge voltage yields decreased structural disorder, i.e. a lower C–C sp^3 hybridised fraction of carbon atoms in the films. By an elevation of the discharge voltage from 1 to 3 kV the full width at half maximum of the G-band decreases from 194 ± 0.2 cm^{-1} to 183 ± 0.7 cm^{-1}. Films deposited at the lowest discharge voltage show in accordance to the spectroscopic data the highest nanohardness (36 ± 1 GPa), stress (-2.34 ± 0.2 GPa) and reduced elastic modulus (180 ± 4 GPa).

1. Introduction

Diamond-like carbon (DLC) films, which present a metastable form of carbon in an amorphous structure with a mixture of sp^2 and sp^3 hybridised bonds, have a wide range of applications. Initially, the films played an important role for tools or engineering components as wear resistant coatings, ensuring high hardness and low friction coefficients [1,2]. Wear protection is still one of the main implementations of DLC coatings, whereas in recent years these films have become more and more relevant as barrier coating on artificial implants, stents or applications in analytical chemistry, for example as corrosion-resistant coating on zinc selenide infrared waveguides [3]. Moreover, biochemists have found DLC as a useful functional surface for cell biology or immobilisation experiments of proteins [4–6].

Depending on the mechanical and structural needs for application, these films can be deposited by pulsed laser deposition, sputtering, chemical vapour deposition and filtered cathodic vacuum arcs [2]. Each of these named deposition techniques has limitations in several important properties of DLC films, such as the presence of defects, known as particulates and droplets or lacking adhesion on different substrates. For the application of DLC films as corrosion-resistant coatings or coatings on artificial implants in contact with human serum and blood, defect-free layers are mandatory. Methods, where a solid target is sputtered or evaporated by a laser beam do not provide defect-free films. Macro-particles emitted from the target can hit the substrate, generating defects in the growing DLC coating. These macro-particles are also known as the origin of porosity and pinholes, due to shadowing effects and removal of initially adherent macro-particles during film growth.

Deposition techniques, which use gaseous carbon containing precursors for film growth like chemical vapour deposition as well as ion beam methods, have the great advantage of growing basically defect-free films. Veerasamy et al. [7] reported in 2003 on a deposition technique using a closed drift linear ion beam source to deposit hydrogenated tetrahedral amorphous carbon films (ta-C:H) with sp^3 contents as high as 80% directly onto glass substrates. They also claimed excellent adhesion of the ta-C:H coatings on the glass substrates, caused by the initial effect of implantation of carbon into the glass surface enabling the growth of a diffuse interfacial carbon-glass layer [7].

Zhurin et al. [8] have given a detailed review on physics of closed drift thrusters, another field of use and the primal application of linear beam ion sources. Depending on geometrical and material differences, these sources can be divided into magnetic layer thrusters and the so called anode layer types. In general, the electric field that accelerates the ions is established by an electron current that passes through and is guided by a magnetic field [8]. These electrons follow a closed drift path, which is eponymous for these devices. The anode layer thruster has its origin in the acceleration of electrons from the cathode to the anode, increasing the electron temperature, which results in a sharp decrease in plasma

* Corresponding author. Tel.: +43 3842 81260 2303; fax: +43 3842 81260 2310.
E-mail address: markus.kahn@joanneum.at (M. Kahn).

0040-6090/$ – see front matter © 2009 Elsevier B.V. All rights reserved.
doi:10.1016/j.tsf.2009.03.213

potential, so that the ion generation and acceleration takes place in the form of a thin layer near the anode, giving the source its name — anode layer source [8]. The characteristics of an anode layer thruster are that the channel where the discharge takes place is short compared to the width of the channel. Thus, these types of ion sources are also called thrusters with short acceleration zone [8].

In thin film technology, anode layer sources are used for argon or oxygen plasma cleaning of substrates. Such a source can also be fed with hydrocarbon gases to deposit DLC films, as reported by Veerasamy et al. [7]. In this work, we applied a linear ion beam source for DLC deposition in a unique configuration, employing the so called contamination shielding plates installed at the cathodes of the ion source. These shielding plates are constructed to reduce the contaminant uptake from plasma erosion of the cathodes [9]. Using the described shielding plates it is possible to reduce contamination in the growing films for at least 50% [9]. The aim of this study was to elucidate trends in the structure formation and mechanical property evolution of DLC films deposited by an anode layer source with varying discharge voltage, process pressure as well as different substrate manipulation in front of the ion beams using C_2H_2 as precursor gas.

2. Experimental details

2.1. Film deposition

For deposition of DLC films, an ALS340L anode layer source from Veeco Instruments (Woodbury, NY, USA) was fed with acetylene (C_2H_2, nominal purity >99.96%). Fig. 1a shows a sketch of a cross-section of the anode layer source, and Fig. 1b outlines its working principle [9]. The gas was directly introduced into the discharge channel. The anode layer source was powered with a high voltage DC power supply from Glassman High Voltage (High Bridge, NJ, USA) in the voltage controlled mode. Discharge voltages ranging from 1 to 3 kV were applied to the anode, providing ion energies of roughly 450 to 750 eV [9].

Silicon wafers (100) with a thickness of 525 ± 25 µm were used as substrates. The wafers were chemically cleaned in an ultrasonic cleaner sequentially with acetone and ethanol, and were dried with nitrogen. The wafers were fixed on a grounded substrate holding carrousel situated at a distance of approximately 15 cm from the ion source. The diameter of this carrousel was 56 cm whereas the samples were fixed at a diameter of 40 cm on vertical static columns. No substrate bias was used during the depositions. For lateral mappings to investigate the film thickness uniformity as well as structural uniformity, 20 silicon wafers (1 cm broadness with a gap of ~0.9 cm) were mounted horizontally at a distance of 15 cm from the source. Films were deposited in three ways: in static mode, by oscillation of the carrousel with an amplitude of 9 cm (left–right), and by rotation around the vertical axis of the carrousel. The movement was in all cases one-dimensional and perpendicular to the ion beams of the linear anode layer source. The substrate temperature was monitored with an electrically insulated K-type thermocouple installed at the backside of the substrate holder.

For plasma cleaning of the wafers prior to deposition, the ion source was operated at a voltage of 2 kV and an argon (Ar) (nominal purity >99.999%) flow rate of 20 sccm through the ion gun, resulting in a power density of 2.8 W cm^{-1} (power on the anode layer source per cm of the discharge channel). For all depositions, the chamber was evacuated to a base pressure of $\leq 5 \cdot 10^{-3}$ Pa. During deposition, the pressure in the chamber ranged from 0.15 Pa to 0.3 Pa via introducing 10 to 30 sccm of C_2H_2.

2.2. Film thickness and intrinsic stress

Thickness and internal stress of the films were determined using a stylus profilometer Form Talysurf Series 2 from Taylor Hobson Ltd. (Leicester, GB). Step size measurements were carried out at edges of coated and uncoated areas on the silicon substrates. For stress measurements, the wafers were checked for flatness prior to deposition. During deposition, these samples were fixed only on one end so that the wafer could follow the stress emerging during growth of the DLC film. Care was taken to avoid possible coating of these samples at the backside. After deposition of ~1 µm thick films, the curvature on the silicon wafers was measured with a stylus force of 1 mN. The stress in the films was calculated using the modified Stoney equation [10].

2.3. Vickers microhardness, nanohardness and atomic force microscopy

Vickers microhardness of DLC films with ~1 µm thickness was measured with a Fischerscope H100C from Helmut Fischer (Sindelfingen-Maichingen, Germany) using a Vickers indenter and loads ranging from 3 to 10 mN. The indentation depth ranged from 10 to 20% of the coating thickness for the applied loads. The hardness and elastic modulus showed relative standard deviations of less than 10% for all loads used, so that in the following figures data from the 3 mN measurements are presented. In addition, on films with a thickness of ~200 nm, nanoindentation measurements were carried out on a Hysitron Triboscope (Hysitron Inc., Minneapolis, MN, USA) using a cube-corner indenter with a tip radius <50 nm. Quantitative hardness and reduced modulus values were determined from the unloading part of the load–displacement curves, applying the method introduced by Oliver and Pharr [11]. The reduced modulus takes into account the deformation of the indenter tip and the lateral deformation of the sample material via its Poisson's ratio [11]. At constant indention depth on each film the relative standard deviation of hardness and modulus did not exceed 3%. Effects like the influence from the substrate [12] and

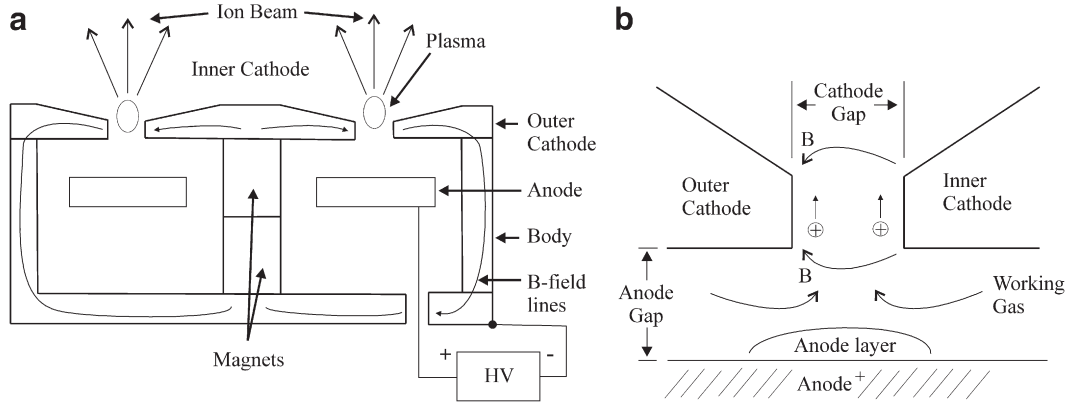

Fig. 1. a) Cross-section of the anode layer source ALS340 from Veeco Instruments showing the main components of the source body and electrical circuit points (after [9]). b) Working principle of the anode layer source (after [9]).

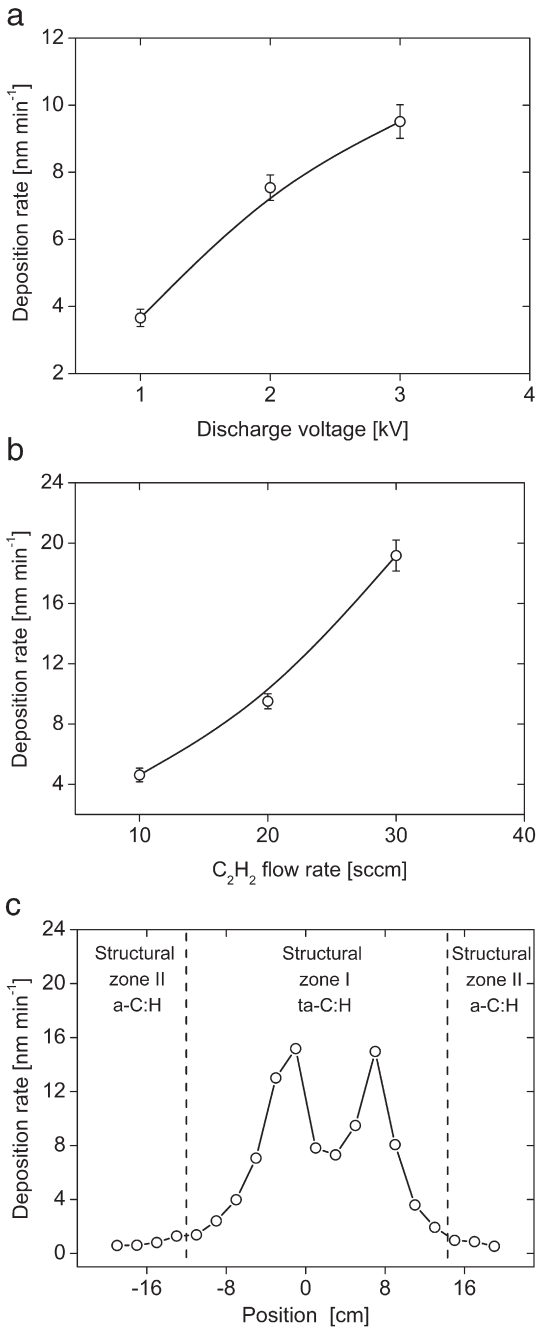

Fig. 2. Deposition rate as function of a) discharge voltage at constant C_2H_2 flow of 20 sccm, b) C_2H_2 flow rate at constant discharge voltage of 3 kV, and c) the horizontal position perpendicular to the beam major axis. Additionally, structural zones I and II are shown, which are discussed in the text.

indentation size effect [13,14] were excluded by a careful choice of the indentation depth. In order to check a possible influence from the substrate, loads ranging from 200 to 750 μN were applied. For the determination of surface roughness, atomic force microscopy (AFM) imaging was performed using an ultra-sharp, high-aspect ratio tip in tapping mode with a scan size of 5 × 5 μm.

2.4. Micro-Raman spectroscopy

A HR 800 high-resolution Raman microspectrometer from Jobin-Yvon (Villeneuve d'Ascq, France) was used to characterise the structure of carbon bonds in the DLC films. The instrument was operated with lasers at excitation wavelengths of 325, 532 and 633 nm, respectively. Olympus 40× (for 325 nm) and 100× objectives (for 532 and 633 nm) were used to focus the beams on the sample, where in all cases the power of the laser was kept well below 0.25 mW. The entrance slit to the spectrometer was set to 100 μm and holographic gratings with 1800 grooves mm^{-1} were used for 532 and 633 nm and 2400 grooves mm^{-1} for 325 nm excitation. A standard (100) orientated silicon wafer with a Si-peak position of 520 cm^{-1} was used as drift standard for all excitation wavelengths. A resolution of 0.3 cm^{-1} could be achieved with the spectrometer. Mathematical spectrum fitting for the D and G-bands with Gaussian functions was performed with "Peak-Fit" 4.11 from Systat (Point Richmond, CA, USA). Additionally, Raman spectra of films deposited at the lowest ion energy were fitted with a Breit–Wigner–Fano function (BWF) for the G-band and a Lorentzian for the D-band. The G-band in Raman spectra from amorphous carbon phases taken at visible excitation has its origin in the effect of bond stretching of all carbon atoms in sp^2 hybridisation in rings and chains. The D-band occurs from the breathing mode of carbon atom rings [15–17]. I_D/I_G ratios were calculated by using peak heights. Since this work focuses on the spectral features of the D and G-bands, other Raman active modes have been neglected.

3. Results and discussion

3.1. General film properties

In order to investigate the influence of C_2H_2 flow and discharge voltage on the deposition rate of the DLC films, we performed experiments by varying the C_2H_2 flow from 10 to 30 sccm while keeping the discharge voltage constant at 3 kV. In addition, investigations were carried out by varying the discharge voltage from 1 to 3 kV while working with constant C_2H_2 flow of 20 sccm (at constant substrate oscillation). The results show an increased deposition rate with higher discharge voltage (Fig. 2a): A deposition rate of 3.7 ± 0.3 nm min^{-1} was found for 1 kV and 9.5 ± 0.5 nm min^{-1} for 3 kV. Besides this, elevating the C_2H_2 flow through the source by a factor of three resulted in a fourfold increase of the deposition rate (Fig. 2b).

Static deposition experiments with the standard C_2H_2 flow of 20 sccm and an applied discharge voltage of 3 kV showed the expected spikes of deposition rate in front of the two plasma beams of the anode layer source (Fig. 2c). The observed profile of the deposition rate corresponds to the particle density of the two beams. Working with oscillation amplitude of 9 cm showed a symmetric and homogeneous deposition rate of 9.5 ± 0.5 nm min^{-1} over a horizontal distance of approximately 10 cm using similar process conditions.

A great advantage of this deposition process is the low temperature of the substrates of less than 70 °C after runs for several hours with the highest possible discharge voltage of 3 kV. Depositions at 1 kV discharge

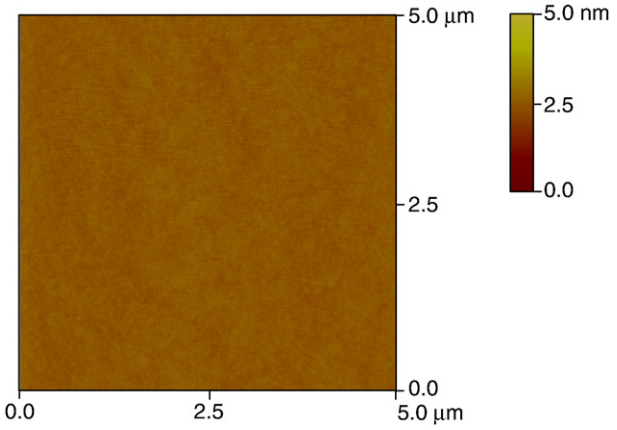

Fig. 3. AFM image of the DLC surface.

voltage showed an equilibrium temperature of less than 40 °C on the substrates. Hence, this technique of depositing DLC films is very versatile and can be applied also on temperature-sensitive substrates.

Another advantage is the smooth and defect-free DLC surface obtained by this method. AFM studies on our deposited films showed a roughness of the DLC surfaces of 0.1–1 nm. Fig. 3 shows an AFM image of the smooth and homogeneous surface. With such highly defect-free films it is possible to realize much thinner and compact coatings compared for example to sputtered DLC coatings. It might thus be assumed that our coatings are comparable to those applied in semiconductor industry, where DLC films with thicknesses as thin as 1 nm are used for protective coatings of data storage materials, deposited with gridless ion source technology [1].

3.2. Structural properties

Fig. 4 shows an exemplary Raman spectrum (with additional Gaussian function fits for the D and G-band), taken from a film deposited with 20 sccm C_2H_2 at a discharge voltage of 1 kV (at constant substrate oscillation). The bands were found to be at spectral positions of 1358 ± 2 cm^{-1} (D-band) and 1541 ± 1 cm^{-1} (G-band). In order to describe the structure of the films it is necessary to discuss the intensity ratio I_D/I_G, the full width at half maximum of the G-band (FWHM (G)), the position of the G-band and the dispersion of the G-band with excitation wavelength. First, it has to be considered, that the intensity ratio I_D/I_G is a measure of the size of the sp^2 phase organized in rings [18]. If the intensity ratio I_D/I_G becomes lower or zero, the sp^2 phase is organised rather in chains, whereas a higher intensity ratio I_D/I_G is an indication of an increase of the sp^2 phase in aromatic rings. Thus, if no D-band is visible, no sp^2 carbon rings exist in the material [15].

For hydrogenated amorphous carbon films (a-C:H), where the sp^2 phases and the sp^3 phases are linked together, the visible Raman parameters (532 nm) can be used to reveal information about the sp^3-hybridisated carbon fraction of the films. A lower intensity ratio I_D/I_G is connected with higher overall sp^3 content [15,16]. Since carbon is sp^3 bonded in a-C:H films also to hydrogen, an increase in sp^3 content does not always mean an increase in density, hardness and other mechanical properties [15,18]. For a-C:H with hydrogen contents over 25 at.% the overall sp^3 content can increase, but not the C–C sp^3 content. Such polymeric films have the lowest hardness, stress and density. The ta-C:H films represent a class of hydrogenated DLC in which the C–C binding content can be increased while keeping a fixed hydrogen content (25 to 30 at.%) [18]. Therefore ta-C:H have much more C–C sp^3 bonding than a-C:H, enabling a higher hardness and density while having a similar sp^3 content as an a-C:H film [15,18]. Thus, utilizing the intensity ratio I_D/I_G only, it is difficult to estimate the bonding regimes in amorphous carbons. To investigate the structure of the deposited films in more detail it is necessary to focus also on the FWHM (G). The FWHM of the G-band is a key parameter of monitoring structural disorder in DLC films [18]. This structural disorder arises from the bond angle and bond length distortions in DLC. The FWHM (G) is small when sp^2 clusters are more defect-free and ordered and a higher FWHM (G) is thus indicative for an increase in disorder [18]. The effect originates in the higher bond length and higher bond angle in more disordered material [18]. The increase in disorder is here linked to an increase in C–C sp^3 content, density, and hardness [18]. Casiraghi et al. [18] stated, that this concept holds for hydrogen free carbons as well as for a-C:H with hydrogen contents around 20–30 at.%. At higher hydrogen contents, FWHM (G) as an indicator for structural disorder decreases for a-C:H with hydrogen contents higher than the prementioned 30 at.% [18].

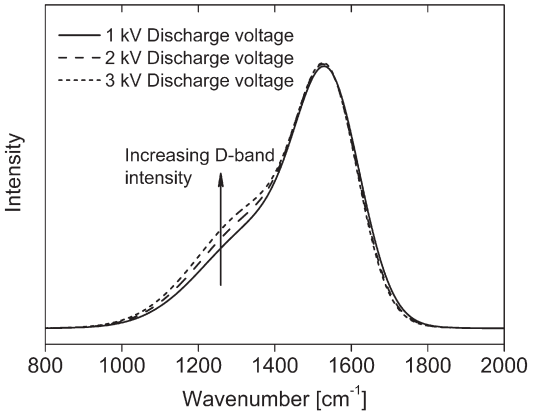

Fig. 5. Raman spectral shape as function of discharge voltage measured at 532 nm.

An I_D/I_G ratio of 0.48 ± 0.02 was calculated with peak amplitudes of the bands shown in Fig. 4. Intensities from D and G-bands taken from samples deposited at higher discharge voltages of 2 and 3 kV at similar process parameters show enhanced I_D/I_G ratios of 0.53 ± 0.01 and 0.59 ± 0.01, respectively. Fig. 5 shows the discussed increase in D-band intensity induced by a higher discharge voltage and Fig. 6 depicts graphically the rise in I_D/I_G ratios when increasing the discharge voltage. The position of the G-band shows no significant shifts while increasing the discharge voltage and remains at a constant position of 1541 ± 0.7 cm^{-1}. From these data, a trend of an increased clustering of sp^2 phases in rings for higher discharge voltages can be deduced [15–18]. We did not investigate films deposited at lower discharge voltages since the anode layer source is only stable at a minimum discharge voltage of 0.6 kV. In order to confirm the trends derived from the intensity ratios, the FWHM of the G-band is used to reveal

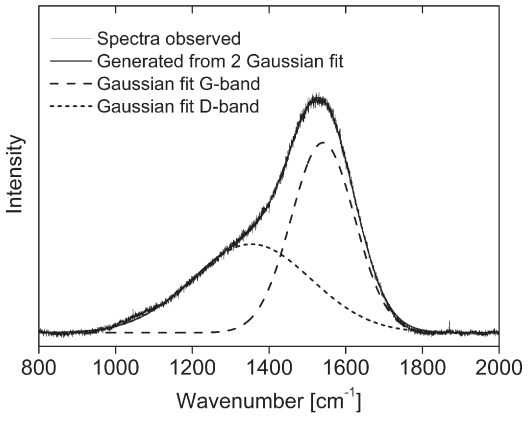

Fig. 4. Exemplary Raman spectrum recorded with 532 nm for an a-C:H coating deposited with 20 sccm C_2H_2 at a discharge voltage of 1 kV.

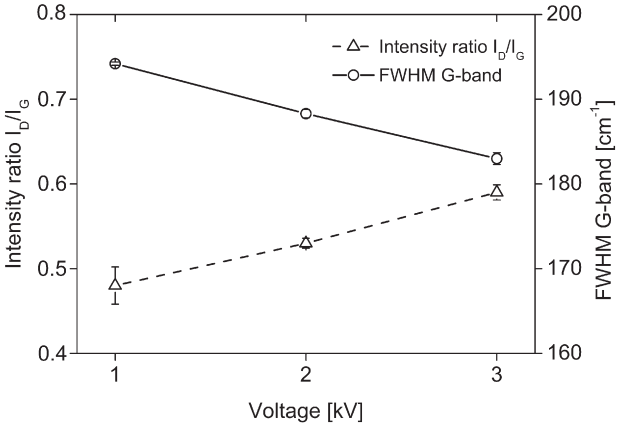

Fig. 6. Intensity ratio I_D/I_G and FWHM (G) as function of discharge voltage (measured at 532 nm).

information about the structural variance induced by changes in the process parameters. For films deposited at a discharge voltage of 1 kV, a FWHM (G) of 194 ± 0.2 cm^{-1} was derived from the Gaussian fits, which decreases linearly to 183 ± 0.7 cm^{-1} for a discharge voltage of 3 kV (Fig. 6). The trends in FWHM (G) completely confirm the observed behaviour that the films at the lowest discharge voltage have increased structural disorder. The increase in disorder can here be linked to an increase in C–C sp^3 content in the material [18]. The high FWHM (G) of 194 ± 0.2 cm^{-1} (fitted with a Gaussian function) for the most disordered film deposited at the lowest ion energy suggests the classification of the deposited film to the structural class of ta-C:H. Additional fitting of the obtained spectra with a BWF function for the G-band and a Lorentzian for the D-band showed a FWHM (G) of 249 cm^{-1} with an I_D/I_G ratio of 0.06. This allows the comparison of our measured data with results from Conway et al., where I_D/I_G ratios of ~0.05 were reported for ta-C:H films [19].

The topological disorder of the deposited DLC films can be probed by Raman measurements with more than one excitation wavelength [18]. The topological disorder arises from the size and shape distribution of the sp^2 clusters. Only a carbon material with disorder shows G-band dispersion, because the dispersion has its origin in the resonant selection of sp^2 chains of different sizes (conjugation length) at different excitation energies [18]. A hydrogenated amorphous carbon film, deposited by using a C_2H_2 flow rate of 20 sccm at a voltage of 3 kV (at constant substrate oscillation), was investigated with excitation wavelengths of 633, 532 and 325 nm, respectively. The position of the G-band increases from ~1516 cm^{-1} to ~1588 cm^{-1} while lowering the excitation wavelength. The dispersion is 0.23 cm nm^{-1} for the investigated film, which fits well the results in literature for dispersion of a-C:H [18].

Evolution of the background slopes arising in the spectra showed unaffected backgrounds with no increasing photoluminescence caused by elevated hydrogen contents in DLC films when using a relatively high excitation wavelength of 532 nm in Raman spectroscopy [15]. The Raman spectra indicate a hydrogen content of roughly ≤25 at.%, which could be estimated from the ratio of the fitted background slope (m) per intensity of the G-band (I_G) [15] of ~0 μm. This result authenticates that the anode layer source is able to decompose the C_2H_2 molecule for growing a-C:H films with roughly ≤25 at.% hydrogen when using the described experimental setup.

We want to highlight, that a deposition with a static mapping, where 20 silicon wafers were mounted perpendicular to the major beam axis of the source, showed increased m/I_G ratios up to 10 μm at a horizontal distance of approximately 10 to 12 cm (measured with 532 nm excitation) from the axis of the source. This indicates a higher hydrogen concentration in the films, which causes the increased m/I_G ratio in the Raman spectrum [15]. These films are authentic a-C:H films which showed a decreased FWHM (G) down to ~140 cm^{-1}. Fig. 2c depicts the zones (zones II (a-C:H)), where these strongly hydrogenated films can be found. It can be assumed, that these films have lower structural disorder which is estimated by the decreased FWHM (G). Samples mounted to the prementioned distance of up 10 to 12 cm showed no increased slope of the Raman spectra background which gives values for m/I_G of ~0 μm. This structural zone (zone I (ta-C:H)) is shown as well in Fig. 2c. Oscillation as well as complete rotation of the samples through the plasma beams showed in all cases ratios for m/I_G of ~0 μm.

Further Raman investigations showed also a dependence of the FWHM (G) and the I_D/I_G ratio of the films as a function of the horizontal position perpendicular to the major beam axis. A discharge voltage of 3 kV and a C_2H_2 flow of 20 sccm were applied for this investigation. A FWHM (G) of 190 ± 0.5 was detected for samples which were installed between the two plasma beams. A lower FWHM (G) of 182 ± 1 cm^{-1} measured for samples installed directly in front of the two beams evidenced the proposed behaviour, that higher ion energy yields less tetrahedral character films with less disordering.

Additionally, the I_D/I_G ratio was used to verify the structural trends derived from the FWHM (G) for these experiments. An I_D/I_G ratio of 0.48 ± 0.07 was detected for samples installed in front of the center of the source, whereas an I_D/I_G ratio of 0.6 ± 0.02 was observed for samples positioned directly under the beams. This observation confirmed that higher ion energies on samples immediately in front of the two beams result in an increased clustering of sp^2 phases in the DLC films, also known as an ordering process. Furthermore, this guarantees the described overall behaviour that films grown with generally higher discharge voltages of 3 kV show less C–C sp^3 fractions. The I_D/I_G ratio of 0.48 ± 0.07 in the lower ion energy region in the center of the source between the two plasma beams is similar to the results observed for processes with oscillating movement of the substrates where the discharge voltage was set to 1 kV.

We also investigated the influence of mixing Ar to the process gas in order to find further improved deposition parameters. These experiments were carried out with the standard procedure of oscillating the silicon wafers with an amplitude of 9 cm through the ion beams. The total gas flow was 20 sccm and the discharge voltage for these experiments was set to 1 and 3 kV, respectively. With a mixture of 15 sccm C_2H_2 and 5 sccm Ar, an I_D/I_G ratio of ~0.60 was detected for a discharge voltage of 1 kV. A discharge voltage of 3 kV with similar conditions showed a further increased I_D/I_G ratio of ~0.80. The FWHM (G) decreased from ~190 to ~176 cm^{-1} when increasing the discharge voltage from 1 to 3 kV. Introducing mixtures of Ar and C_2H_2 into the anode layer source showed an ordering process in the DLC films. This behaviour can be interpreted as the result of the high energy ion bombardment by heavy Ar-ions during film growth, reducing the disordered character and C–C sp^3 content. It can be concluded that highly disordered films can be achieved by using exclusively C_2H_2 as process gas. It is also reported by Conway et al. [19] that C_2H_2 is the favoured precursor for growing ta-C:H with plasma beam methods. They report, that depositions, where methane as carbon source is used, do not grow authentic ta-C:H and the character is less tetrahedral [19].

3.3. Mechanical properties

In order to validate the structural trends derived from Raman spectra, we applied the nanoindentation method to 200 nm thick films. The nanohardness increased with decreasing discharge voltage and ion energy (Fig. 7). A nanohardness of 36 ± 1 GPa and a reduced modulus of 180 ± 4 GPa are indicative for a highly disordered film deposited in our study using the lowest possible ion energy. [2]. It can be concluded that the mean ion energy in our deposition process has the most important influence on the structure of the films.

The results of our study agree well with the results from Weiler et al. [20]; they showed that films deposited with an ion energy of

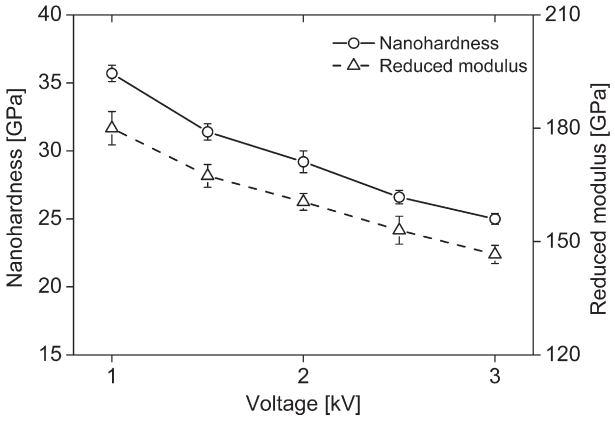

Fig. 7. Nanohardness and reduced modulus as function of discharge voltage.

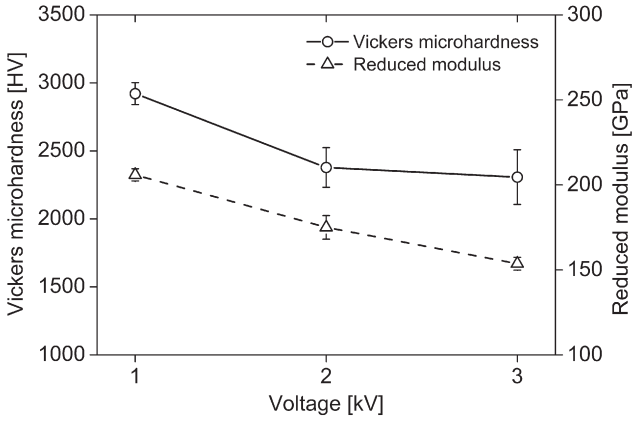

Fig. 8. Vickers microhardness and reduced modulus as a function of discharge voltage.

~90 eV per carbon ion using the plasma beam source have the highest C–C sp^3 content. However, Veerasamy et al. [7] found the highest hardness values for mean ion energies of ~750 eV per carbon atom for films deposited on soda-lime glass. They did not observe any drop in hardness and tetrahedral character of the deposited films when working with ion energies up to 1 keV per carbon atom. The ta-C:H films in their study were deposited with a linear ion beam source which is constructed according to the principles of an anode layer source, having a short discharge channel compared to the width of the channel. This source belongs to the short acceleration zone ion guns, as well as the anode layer source we used. Veerasamy et al. [7] report a completely inverse trend of the hardness as a function of the mean ion energy per carbon atom compared to other studies [2,20] as well as our data reported in this paper. They named two possible reasons for higher disordered character of the DLC films deposited at elevated ion energies: First, the presence of H during the film growth may delay the onset of graphitisation which is caused by thermal spikes at high energies, and second, the charging of the film surface can also reduce the effective energy of the incident ions. In contrast, our films show highest hardness and disordered character when working with the lowest possible ion energy. In order to establish further evidence of our results from nanohardness measurements, we applied the Vickers microhardness method to films with enhanced thicknesses of ~1 µm. The results are plotted in Fig. 8. A Vickers microhardness of 2900 ± 80 HV could be detected for the film deposited by the lowest discharge voltage of 1 kV. The Vickers microhardness also confirmed the trend derived from our nanohardness results that increased ion energy yields less disordered character and less hardness.

The trends derived from Raman spectroscopy and nanoindentation could also be fully evidenced by the determination of stress in our films. The stress in DLC is known to increase with increasing C–C sp^3 binding content [2]. The measured values showed the expected drop in compressive stress when increasing the discharge voltage. For a discharge voltage of 3 kV, a compressive stress of -0.85 ± 0.02 GPa was detected, whereas the films deposited at 2 and 1 kV showed -0.89 ± 0.3 and -2.34 ± 0.2 GPa, respectively.

4. Conclusions

The present paper demonstrates the unique properties of an anode layer source for the direct deposition of hard a-C:H films. Raman spectra indicate an increasing disorder of the film structure when applying the lowest ion energy for film growth. This behaviour is confirmed by elevated hardness, reduced modulus and intrinsic stresses in films deposited at the lowest ion energy. Due to the very smooth and defect-free nature of the deposited a-C:H films, these films are assumed to be excellent candidates for applications as corrosion-resistant coatings or coatings of artificial implants.

Another important benefit of this coating technique is a low substrate temperature of <70 °C, which makes the method very versatile for coating of temperature-sensitive surfaces. We want to highlight the simple and robust working principle of the anode layer source, which enables the use of the source for plasma cleaning of substrates as well as for deposition of a-C:H films for industrial applications.

Acknowledgements

Financial support of this work by the Austrian Federal Ministry of Traffic, Innovation and Technology, the Austrian Industrial Research Promotion Fund (FFG), the Government of Styria, Forschung Austria and the European Union is highly acknowledged.

References

[1] A.C. Ferrari, Surf. Coat. Technol. 180–181 (2004) 190.
[2] J. Robertson, Mater. Sci. Eng. R37 (2002) 129.
[3] M. Janotta, D. Rudolph, A. Kueng, C. Kranz, H.S. Voraberger, W. Waldhauser, B. Mizaikoff, Langmuir 20 (2004) 8634.
[4] F.Z. Cui, D.J. Li, Surf. Coat. Technol. 131 (2000) 481.
[5] T. Yokota, T. Terai, T. Kobayashi, M. Iwaki, Nucl. Instrum. Methods Phys. Res. B 242 (2005) 48.
[6] C. Lim, S. Slack, S. Ufer, E. Lindner, Pure Appl. Chem. 76 (2004) 753.
[7] V.S. Veerasamy, H.A. Luten, R.H. Petrmichl, S.V. Thomsen, Thin Solid Films 442 (2003) 1.
[8] V.V. Zhurin, H.R. Kaufman, R.S. Robinson, Plasma Sources Sci. Technol. 8 (1999) R1.
[9] Veeco Instruments, Technical Manual to ALS340, 2003.
[10] G.G. Stoney, Proc. R. Soc. Lond. Ser. A82 (1909) 172.
[11] W.C. Oliver, G.M. Pharr, J. Mater. Res. 1 (1992) 1564.
[12] T. Staedler, K. Schiffmann, Surf. Sci. 482–485 (2001) 1125.
[13] W.D. Nix, H. Gao, J. Mech. Phys. Solids 46 (1998) 411.
[14] K. Durst, B. Backes, M. Göken, Scripta Mater. 52 (2005) 1093.
[15] A.C. Ferrari, J. Robertson, Philos. Trans. R. Soc. Lond. Ser. A 362 (2004) 2477.
[16] A.C. Ferrari, J. Robertson, Phys. Rev. B 61 (2000) 14095.
[17] A.C. Ferrari, J. Robertson, Phys. Rev. B 64 (2001) 075414.
[18] C. Casiraghi, A.C. Ferrari, J. Robertson, Phys. Rev. B 72 (2005) 085401.
[19] N.M.J. Conway, A.C. Ferrari, A.J. Flewitt, J. Robertson, W.I. Wilne, A. Tagliaferro, W. Beyer, Diamond Relat. Mater. 9 (2000) 765.
[20] M. Weiler, S. Sattel, T. Giessen, K. Jung, H. Ehrhardt, V.S. Veerasamy, J. Robertson, Phys. Rev. B 53 (1996) 1594.